MASCOT - STRUCTURES DESIGN AND QUALIFICATION OF AN "ORGANIC" MOBILE LANDER PLATFORM FOR LOW GRAVITY BODIES

Michael Lange [(1)], Olaf Mierheim [(1)], Christian Hühne [(1)]

(1) German Aerospace Center, Inst. of Composite Structures and Adaptive Systems, Lilienthalplatz 7, 38108 Braunschweig, Germany, Email: m.lange@dlr.de

ABSTRACT

The DLR Mobile Asteroid Surface Scout (MASCOT) is an approx. 10kg shoebox-sized lander platform developed in cooperation with CNES and JAXA for the Hayabusa 2 Asteroid Mission heading to the C-class asteroid 1999 JU3. MASCOT carries four scientific instruments as well as a mobility mechanism for up righting and relocation on the asteroid during autonomous operation. The MASCOT system is subdivided in two main structural composite parts, the Landing Module (LM), housing all experiments and sub-systems, and the Mechanical and Electrical Support Structure (MESS). It provides the LM's interface to Hayabusa 2 until separation. This paper provides an insight into the structural design concept, development and corresponding mechanical flight qualification for both parts.

1. INTRODUCTION

The DLR Mobile Asteroid Surface Scout (MASCOT) is an approximately 10kg shoebox-sized lander platform developed in cooperation with CNES and JAXA for the Hayabusa 2 sample return mission heading to the Cg-class asteroid 1999 JU3 [1]. MASCOT is dedicated to support Hayabusa 2 with landing site selection and to enhance it with in-situ surface science capabilities. Therefore it carries four instruments weighing a total of 3kg (see Figure 2). These are MicrOmega (near-infrared hyperspectral microscope), Cam (camera in visible range), MARA (radiometer) and MAG (magnetometer). For the purpose of up righting and relocation on the asteroid's surface the lander's common electronic box (E-Box) houses a mobility mechanism, which is based on a tungsten mass eccentrically mounted at the end of a step motor-driven momentum arm. Further the E-Box provides on its top side a late access interface for the battery sub-system, which provides for 16 hours electrical power during MASCOT's operational phase on the asteroid's surface. 16 hours correspond to two asteroid days.

The MASCOT system itself is subdivided in two main structural parts (see Figure 1 and in [2]), the box-shaped Landing Module (LM), housing all experiments and sub-systems, and the surrounding Mechanical and Electrical Support Structure (MESS). Both are constructed as highly stiff and lightweight composite framework structures having together a total mass of around 1.4kg. This paper gives an insight view into their structural design concept. FEM (Finite Element Method) and measurement results (acceleration sensors and strain gauges) gained in the mechanical qualification tests on system and subsystem level are presented. By comparing FEM calculation and measurements, the dynamic coupling and decoupling of the structural parts/components can be followed. Exemplarily the MESS is discussed in more detail, which highlights the different design stages and adaptions based on test results. The influence of the different designs on the static and dynamic system behaviour is also shown.

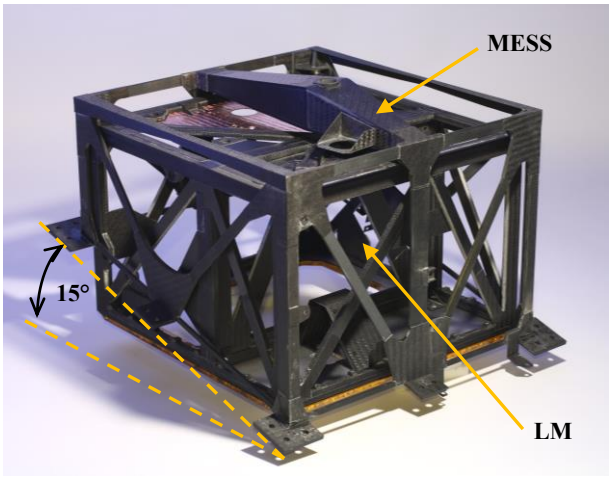

Figure 1. MASCOT LM & MESS FM structures.

2. STRUCTURAL CONCEPT

MASCOT system is composed of two main structural parts, LM and MESS. While the LM is the actual instrument carrying platform, the MESS serves as body fixed interface structure to Hayabusa 2 mother spacecraft. It has a dedicated rectangular cut-out in the upper part of its -Y-plane underneath the left-hand side fixed solar array. This results directly into two main requirements for the mounting concept of the MASCOT system (see also in [2]):

1. Negative inclination of 15° to the –Y-panel.
2. MASCOT system shall not protrude more than 80mm out of Hayabusa 2 Y-Plane.

The next sections, further describes the structural design of the LM and the MESS.

2.1. Landing Module

The LM is designed as a framework structure based on separate CFRP/foam sandwich walls. Each wall (5mm foam core plus unidirectional CFRP face sheets) is connected to the adjacent one via shear straps.

Proc. '13th European Conf. on Spacecraft Structures, Materials & Environmental Testing', Braunschweig, Germany, 1–4 April 2014 (ESA SP-727, June 2014)

Accordingly the structural design makes maximal use of the highly orthotropic material properties. Only the removable radiator plate is designed as an aluminium sandwich, mounted with screws to the other walls. Table 1 lists the materials used for LM and MESS.

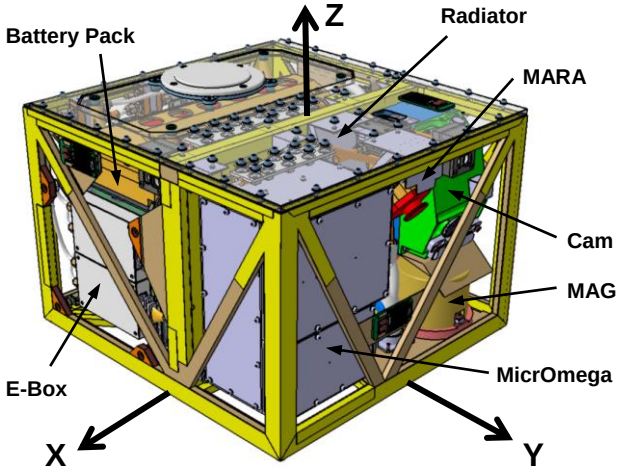

Figure 2. LM Accommodation (radiator in transparent).

The main load for the LM is introduced into the X/Z-Middle Wall plane (see Figure 3, red highlighted) by a separable bolt, connection the LM with the MESS I/F structure. This pulling force of 2500N is guided through the sandwich framework to the bearing points in the four corners of the LM's Bottom Plate, the other interface to the MESS (see [2] and Chap. 2.2). Also the (reaction) forces of payloads (P/L) and heavier sub-units weighing > 0.5kg are only introduced in the wall's in-plane directions. According to the poor out-of plane (OOP) properties of the sandwich framework this leads to a design, which ensures that P/Ls and sub-units are mostly fixed to more than one I/F-wall. For example the E-Box is mounted to two opposite side walls and the Bottom Plate (see Figure 3). The struts of LM's framework walls are partially "wrapped" by two CFRP U-profile forming a rectangle in cross section. This is mainly to stiffen and strengthen the struts in OOP direction.

2.2. Mechanical and Electrical Support Structure (MESS)

The MESS structure is also a framework design making use of the highly-orthotropic CFRP material properties. Unlike the separate sandwich walls as for the LM, MESS has 3mm thick solid quasi unidirectional struts, i.e. it contains 4 layers with ±45° direction. These are again interconnected with shear straps among each other. Main function of the MESS is to mount the LM in its required position on Hayabusa 2. Therefore it is fixed at its lower side with 6 feet to the Hayabusa 2 -Y-Panel. From there the load path is through the framework struts to LM's four counterpart bearings in the upper-sided MESS corners. The stainless steel bearings (see Figure 11 and Figure 12) are designed as a quasi-simply-support and are themselves form shaped glued to dedicated stacked CFRP supports. The physical connection is realized by a central bolt, pulling the LM with 2500N into the bearings. For required thermal insulation the feet are insulated via PEEK (polyetheretherketone) insulators against Hayabusa 2 (see also Chap. 4.1). On the upper side the MESS has a central sandwich truss, which houses the umbilical connector and the spring actuated push-off mechanism.

Part/Component	Material
LM Walls	M55J/LTM123 + Rohacell IG-31F
LM Wall Connectors (Shear Straps)	M40J/Scheufler L160-H163
Radiator	EN AW 6082-T651 + Plascore PAMG-XR1-3.1-18-0007-P-5052
MESS Struts	M55J/LTM123
MESS Strut Connectors (Shear Straps)	M40J/Scheufler L160-H163 & CCC Style 461/Scheufler L160-H163
MESS Main Truss	M55J/LTM123 + Rohacell IG-31F

Table 1. LM & MESS material composition.

3. Finite Element Model (FEM) & Results of siumulation

Both, MESS and LM structures are simulated in MSC.Patran. For the LM, mostly quadratic shell elements (Quad4) and a few triangular shell elements (Tria3) – due to meshing reasons – are used. The MESS is simulated with beam elements and a few additional shell elements representing the main truss' sandwich (see Figure 3). The properties of the solid mess struts are given directly to the beam elements. The shells of the LM walls are simulated by a composite layup including the foam core. Therefore the Patran.Laminate Modeler is used. Both structural parts are interconnected by rigid RBE2 elements (multipoint constraint) which represent the bearing points in the 4 corners.

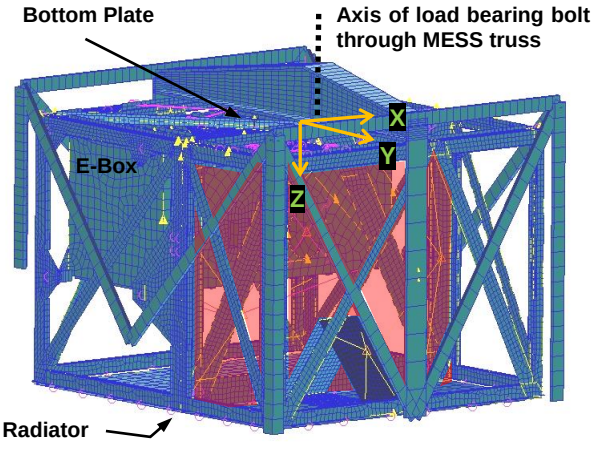

Figure 3. LM & MESS FE Model.

To ensure that the bearings are loaded by a compression load while being pulled together by the central bolt, it is simulated in the Z-direction with two equal forces in

opposite direction. One is acting on the MESS, other on the LM. These simulate the tension by the central bolt with no extra outer force acting on MASCOT system. The force is assumed to be of 2500N. For the rotational degrees of freedom (DOF) around X- and Y-axis as well as the translational DOF in X- and Y-axis a multipoint constraint is used. The LM/MESS bearings, while under pressure load, provide translational fixation in all DOF. Only rotational DOF are free. The eight MESS feet are not detailed represented in the FE model, connecting all the structure to Hayabusa 2 panel. Here the beam elements are clamped in the model. All P/L is considered as a mass point, rigidly connected to the LM structure by RBE2 elements.

The Finite Element simulation covers static (strength and stability) as well as dynamic analyses. Table 3 shows the results of the modal analysis. Most interesting modes are mode 2 (140.7Hz), mode 3 (150.0Hz) and mode 6/7 (175.0Hz/180.3Hz). Mode 2 is triggered by MicrOmega, resulting in a combined movement of the structure in X-axis respectively around Z-axis. This is explained by the low OOP-stiffness of the single struts and local load introduction. The instrument is basically excited in Middle Wall plane, i.e. in X-direction. But due to MicrOmega's centre of gravity (CoG), which has a significant offset to the middle wall, a circular movement is excited at the same time. The same, only with less mass, is valid for Cam, mounted next to MicrOmega on the other half of the Middle Wall. The global Z-mode - mode 3 at 150.0Hz – is triggered by the E-Box and Battery Pack, which is mounted on top. Analogous to mode 2, mode 3 is strongly combined with a circular movement around the Middle Wall, being very stiff in X/Z-plane and so behaving as another bearing. E-Box and Battery Pack bend so the whole structure around it (while simply supported at the bearing corners) by moving Z-Y-wards. Finally the global Y-mode at 180.3Hz (mode 7) is again a combined movement of Camera and MicrOmega. It falls very close with mode 6, a MicrOmega mode only. The results of static FEM calculations are not presented in detail. Both strength and stability analysis showed positive margin for a 50g loading in each direction.

4. Static and dynamic qualification

Exemplarily for the development of the MASCOT structure this paper discusses two crucial stages of static and dynamic qualification. These are: (1) Reaching 1st system Eigen frequency (EF) greater than 120Hz – (2) Strength of MESS bearing corners.

Both were investigated in several tests and design iterations at the structural-thermal model (STM) as shown in the following.

4.1. Dynamic Testing

A first system EF>120Hz was important to reach in MASCOT's structural development and so formed a major design driver. Fulfilling this requirement allowed waiving 25g sine testing (steep ramped and subsequently constant up to 100Hz) on MASCOT system level. In this case only random (and shock testing) was required. The corresponding qualification environment is given in Figure 4 and the setup for Random Vibration test in Figure 5.

Considering the extremely stiff structures and lightweight MESS and LM structures a first EF>120Hz was easily reached. However, especially their lightweight and highly orthotropic design is at the same time problematic, because the major P/Ls' masses are heavy compared to total system mass (Table 2).

Component / P/L	Mass [kg]	Mass ratio [%]
LM	0.56	6.9
LM Radiator(s)	0.19	
E-Box	0.73	6.7
MESS	0.67	6.2
P/L-A	2.08	28.6
P/L-B	0.49	
P/L-C	0.27	
P/L-D	0.25	
System	10.82	100

Table 2. Mass and mass fraction of main structural parts and P/L.

In fact only Camera's and MicrOmega's mass together is almost twice the total structural mass of MASCOT system. So the system's dynamics are strongly coupled to the P/Ls dynamics as already seen in Chap.3. Moreover, the MESS is tilted of 15°, which comes with an inherent coupling of Y- and Z-axis. Figure 6 shows the MASCOT STM low level Sine response for all three

MODE NO.	FREQUENCY	T1		T2		T3		R1		R2		R3	
		FRACTION	SUM	FRACTION	SUM	FRACTION	SUM	FRACTION	SUM	FRACTION	SUM	FRACTION	SUM
1	132.35	4,71	4,71	0,39	0,39	2,77	2,77	0,75	0,75	0,53	0,53	2,98	2,98
2	140.72	37,56	42,28	0,50	0,88	0,00	2,78	0,12	0,88	27,51	28,04	48,07	51,05
3	149.98	0,08	42,36	54,83	55,71	18,34	21,11	47,26	48,13	0,17	28,21	1,83	52,89
4	163.09	0,12	42,49	8,66	64,37	4,09	25,21	0,08	48,21	0,21	28,42	0,13	53,02
5	171.97	18,01	60,50	1,77	66,14	0,29	25,50	0,43	48,64	17,06	45,48	4,63	57,65
6	175.03	27,82	88,31	6,30	72,44	2,54	28,04	2,31	50,95	14,73	60,21	28,13	85,78
7	180.34	5,40	93,71	10,11	82,55	8,11	36,15	6,41	57,36	2,91	63,12	4,03	89,81
8	205.76	0,12	93,83	5,52	88,07	11,90	48,05	0,56	57,92	0,00	63,12	0,01	89,82
9	226.18	0,79	94,63	3,66	91,73	6,19	54,24	0,21	58,13	15,31	78,43	0,05	89,87
10	241.43	0,18	94,81	0,02	91,75	4,80	59,04	0,43	58,56	0,58	79,00	0,03	89,90
11	254.21	0,35	95,15	0,78	92,54	23,09	82,13	0,87	59,43	0,76	79,77	0,02	89,92
12	287.04	0,00	95,16	1,04	93,57	12,47	94,59	31,82	91,25	1,10	80,87	0,15	90,07

Table 3. Modal Effective Mass for first 12 Modes.

axes and a mark for the required 120Hz minimum EF on system level. The first global EF in X-direction is at 122.4Hz and in Y-direction at 157.4 Hz. Furthermore it can be noticed that the Y-axis response has in the lower frequency range two small pre-peaks. These are induced by the Mobility Unit and the MESS main beam respectively.

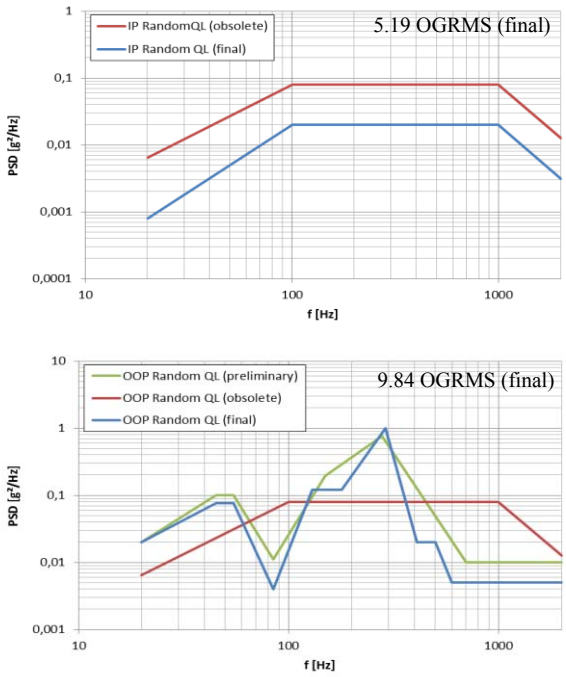

Figure 4. Random QL Environment for MASCOT system. AL = QL -3db.

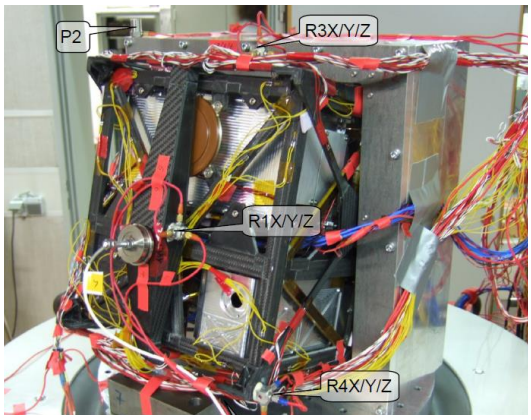

Figure 5. MASCOT MESS & LM STM on shaker for Random Test in y-Direction.

According to FEM simulation the Mobility's EF is below the 120Hz criteria (first mode of a cantilever beam) but at the same time it is very lightweight with respect to the total MASCOT system mass. Due to this a significant influence of the Mobility Unit on the global system behaviour is excluded. The STM Mobility Units' first EF in hard-mounted condition was on sub-system level measured to 119.2Hz, whereas the frequency of the Flight Mobility Unit is even slightly above 120Hz. The second pre-peak at approximately 126Hz can be explained by a local mode of the MESS main truss. That is in Y-direction rather less stiff supported at its axial endings, so it gets excited in this direction at already lower frequencies. The R1 sensor shows here a dominant Y-response. The MESS R4Y sensor in comparison, which is well supported in Y- and X-direction by the diagonal MESS struts, doesn't show this significant behaviour, but only the low pre-peaks and the first global peak in y-direction at 157.4Hz.

In contrast to the Mobility Unit, P/L-"A" has had a significant influence on the overall structural dynamics as shown in the sine response of sensor R4X (see Figure *7*). This P/L was due to thermal reasons flex-mounted first and so driving the first global system EF of MASCOT. This design did not fulfil the 120Hz requirement (red highlighted extract in Figure 7). After changing the P/L's mounting feet design for this and other reasons (thermal requirement turned to be obsolete) a first global system EF of 122.4Hz was reached and so the system requirement fulfilled. The first global EF in Z-direction can be found at 160.2Hz. Comparing the FEM results with the experiment the deviation is obvious. The calculated prediction for X- and Y-direction is 14.7% higher than determined in the experiment. In contrast the Z-direction's 1st EF is 6.7% lower. The reason for this discrepancy can be found in the FE model itself.

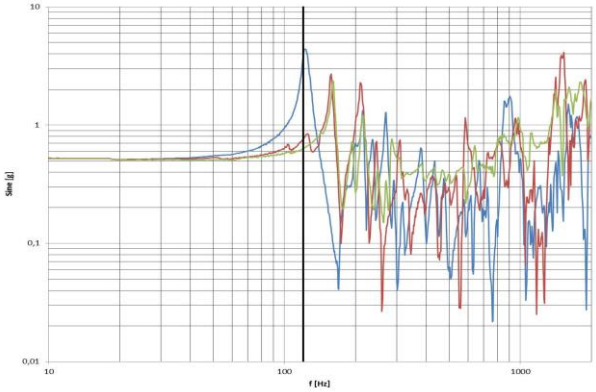

Figure 6. Dynamic coupling on MASCOT STM 2.2. MESS Sensor R4X (blue), R4Y (red) and R4Z (green).

Therein the feet are not modelled in detail (see Chap.3) and the thermal insulators (see Figure 8) are not present, too. The beam endings are clamped at the location of the feet in the real structure. Additionally the FEM doesn't consider a local, rectangular cut-out in the radiator. Here an alone-standing sub-radiator, belonging to the Battery Pack, is placed in the same plane as the main radiator. So the FE model behaves stiffer in X- and Y-direction. In Z-direction this effect can be neglected due to the shaker adapter's support. However an FEM correlation shall be conducted. On MESS, the system's dynamics were studied in detail also separately. Especially the effect of the thermal insulators between MESS feet and Hayabusa 2 -Y-Plane were of interest (see Figure *8*). Accordingly four variants as listed in Table 4 were investigated. The Sine

Response of version (#1) and (#3) is shown in Figure 9 and Figure *10* respectively.

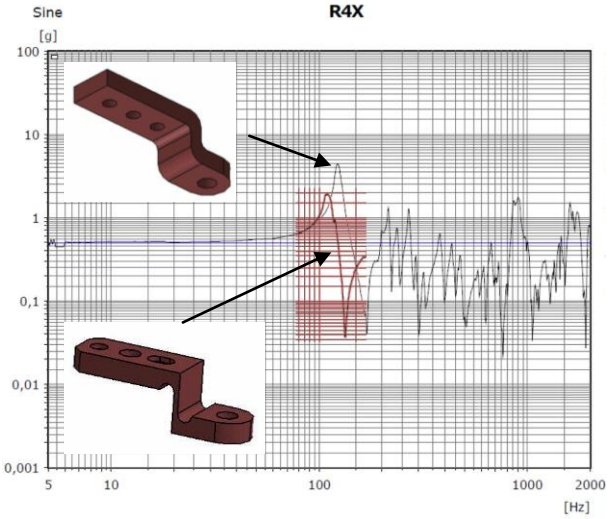

Figure 7. Sine response of sensor R4X (see Figure 5). In red overlaid the influence of P/L-"A" on the 1st system EF w/ 2 different kind of mounting feet.

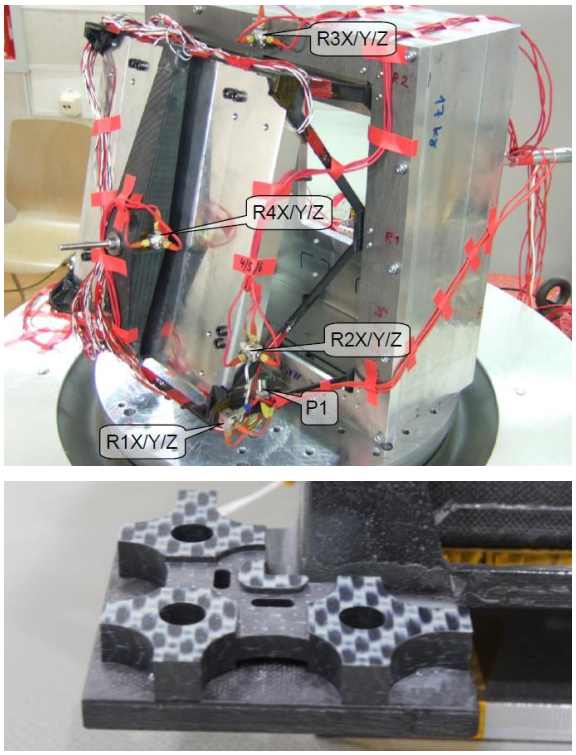

Figure 8. Top: MESS STM 2.1 (y-direction) test setup with 10kg LM dummy and 5mm PEEK insulators. Bottom: Detail of insulator on MESS FS corner foot.

A comparison between the results with 5mm PEEK (#3) insulators and without insulators (#1) reveals their influence on damping and stiffness. While the configuration w/ and w/o PEEK insulators has in the Y-direction a similar first EF (approx. 136Hz), the X- and Z-direction vary significantly. In these directions for both the first EF is of about 15Hz higher without PEEK insulators than with the 5mm ones. Though, due to thermal reasons the insulators are required to have maximal height, i.e. maximal thermal resistance, as cross section is already minimized in contact area. Finally the 5mm PEEK insulators were selected, as with the changes incorporated with MESS STM 2.2 the stiffness was further increased.

Version	MESS Structure	Type of insulator	LM Dummy	Lowest EF
#1	STM 2.1	n/a	10kg	140Hz
#2	STM 2.1	3mm	10kg	125Hz
#3	STM 2.1	5mm	10kg	121Hz
#4	STM 2.2	5mm	10kg	146Hz

Table 4. Insulator versions & results of dynamic stand-alone test with MESS STM 2.X and dummy mass.

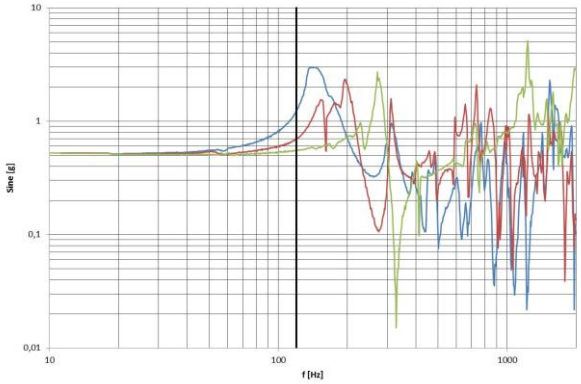

Figure 9. MESS STM 2.1 Sine response w/o PEEK insulators. Sensor R1X (blue), R1Y (red), R1Z (green).

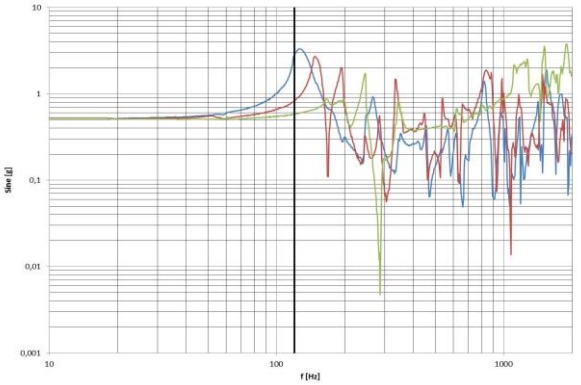

Figure 10. MESS STM 2.1 Sine response w/ 5mm PEEK insulators. Sensor R1X (blue), R1Y (red), R1Z (green).

4.2. Static Testing

Next to the dynamic system and sub-system tests also static tests were performed. For qualifying the structure on system level a static load test of an equivalent load to

23g was required. Furthermore on the MESS a separate sub-system load test was performed in order to verify its structural concept and to cover the even higher loads occurring during random loading with required envelope. So the sub-system test was performed with 3000N in each axis separately. However according to FEM analysis and later to measurements in time frame with strain gauges during random testing the highest load to be expected in the struts is approximately 2500N. Figure 11 and Figure 12 show the –X/-Y-bearing corner of MESS STM 2.1 and FS/FM respectively. They summarise two design changes conducted as a consequence of static load tests.

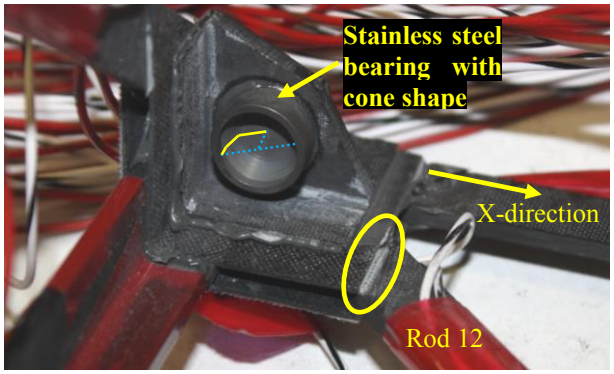

Figure 11. –X/-Y -bearing corner of MESS STM 2.1. Highlighted: Cone shape of stainless steel bearing and crack in the bonding between diagonal strut and bearing corner flange due to too high loading (X-dir.).

Figure 12. –X/-Y -bearing corner of MESS FS/FM with modified diagonal struts' endings and bearing flange.

In Figure 11 a crack in the bonding between the diagonal strut and the bearing corner can be noticed. This occurred during sub-system static load test due to excess of the bonding's shear strength. Consequently, the bonding area was increased by extending the strut's endings and the bearing corner flanges as shown Figure 12. Also to see is the re-designed, hardened stainless steel bearing, which has its counterpart in the LM's corner bearings. First the STM 2.1 bearings have had a less steep cone and no form closure between the stainless steel part and the CFRP bearing corner. At the same time the layup of the CFRP bearing itself was refined for better load transfer into the struts. Further the PEEK insulators at the middle-sided feet were flattened about 0.6mm to pre-load the diagonal struts. A retest with 3000N on STM 2.2 in each direction separately (see Figure 13, X-direction) was successful after applying the mentioned changes.

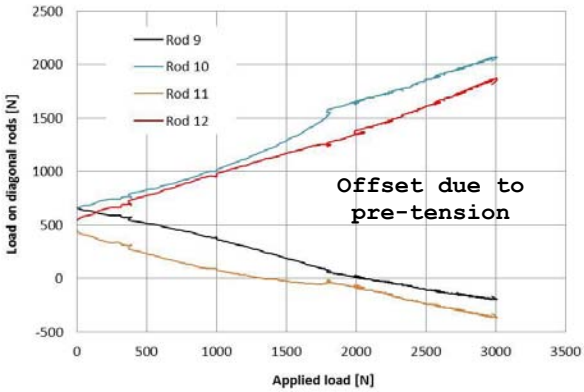

Figure 13. Static Load Test in x-direction on STM 2.2 w/ resulting strut loading (measured via strain gauges).

For final qualification a static load test on system level with 2300N in each direction separately was performed successfully, too. In order to load the system appropriately, total load is subdivided via a momentum free two-staged traverse. It allows distributing the total load via law of momentum arm on each relevant I/F. So E-Box with Battery Pack, Cam and MicrOmega (all mass dummies with a flange in CoG) are loaded at the same time and according to their inertia. The required qualification load is introduced with a step motor and controlled via a load cell in that main load path.

5. Conclusion

With MASCOT, a mobile, very compact ("organic") and lightweight lander structure for low gravity bodies was developed and fully qualified. The paper presented an insight into the LM & MESS structures' development and design. It shows how much the P/Ls and sub-components affect each other as well as the total systems behaviour. Further differences between simulation and tests are analysed. Currently the flight spare and flight unit are undergoing the last system verifications and system integration respectively. In the middle of 2014 the mechanical acceptance test of the MASCOT flight unit on Hayabusa 2 level will take place before it is launched in December 2014.

6. REFERENCES

1. Tsuda, Y. et al. (2013). System design of the Hayabusa 2 – Asteroid sample return mission to 1999JU3. *Acta Astronautica* **91** (2013), pp. 356–362

2. Lange, M. et al. (2012). MASCOT - A Lightweight Multi-Purpose Lander Platform. In Proc. '12th European Conference on Space Structures, Materials & Environmental Testing' Noordwijk, The Netherlands, ESA SP-691 (CD-R)